

FREEZE LINING FORMATION OF A SYNTHETIC LEAD SLAG

Mieke Campforts, Bart Blanpain & Patrick Wollants

Katholieke Universiteit Leuven, Belgium

Evgueni Jak

The University of Queensland, Australia

Tim Van Rompaey

Umicore Research, Belgium

ABSTRACT

Recently, freeze linings have been selected more frequently to protect pyrometallurgical reactor walls, due to a number of advantages over conventional refractory lining such as the self-regenerating capability of the freeze lining and the possibility to operate with intensive process conditions. The freeze linings are formed on the cooled reactor wall in a dynamic time-dependent temperature gradient. A full description of the freeze lining development including phase formation as a function of temperature, time and position therefore is important for understanding the freeze lining formation mechanisms and essential to ensure formation of stable freeze linings. The freeze lining formation is therefore investigated in a synthetic lead slag system $PbO-FeO-Fe_2O_3-ZnO-CaO-SiO_2$. Lab-scale freeze linings were produced by submerging an air-cooled probe into a liquid slag bath for different times from 1 to 120 min. The freeze lining microstructures were characterized with optical and scanning electron microscopy, and with electron probe X-ray micro-analysis. The temperature evolution during freeze lining formation was evaluated with the experimentally determined position and composition of the phases, with the predictions using the thermodynamic computer package FactSage as well as with the results of equilibration experiments.

INTRODUCTION

At present, several processes operate using a cooled reactor wall to extend the life of the refractory. In case of extensive cooling, a layer of process material can solidify on the reactor wall protecting the refractory from corrosion by the process material. This layer is referred to as a freeze lining. For some processes, such as ilmenite smelting [6, 7, 11] and the Hall-Héroult process for the production of aluminium [8, 9], it is very difficult to find suitable refractory material and a freeze lining is the best solution to obtain an acceptable campaign life.

Because the maintenance of this freeze lining has a direct impact on the corrosion of the refractory, it is important to fully understand the freeze lining formation and behavior. In order to control freeze lining stability, an experimental study of the freeze lining microstructure (the phase distribution and composition) is vital. The microstructure determines the properties of the freeze lining and also gives information on the thermal history of the freeze lining.

In previous research, freeze lining microstructures were studied for the Hall-Héroult process [8, 9] and for some industrial nonferrous slags [2, 3, 10]. For the Hall-Héroult process microstructures of industrial freeze linings and lab-scale freeze linings were studied. The main conclusion of the authors was that both the freeze lining microstructure and the freeze lining-bath interface temperature depends on the growth rate of the freeze lining. High growth rates result in the formation of an amorphous layer with limited crystallization and a composition close to the bulk composition. Intermediate growth rates result in dendritical growth of primary phase crystals entrapping bath material. Low growth rates result in a mostly crystalline layer with primary phase columnar crystals and the freeze lining composition is close to the primary phase composition. There is an exchange of components between bath and freeze lining during freeze lining growth. Thus, the composition at the freeze lining-bath interface differs from the bulk bath composition resulting in a different freeze lining-bath interface temperature than the liquidus temperature of the bulk bath. For the industrial nonferrous slags, the freeze lining microstructure strongly changes with distance to the cooled surface and thus with the growth rate of the freeze lining. Different zones are observed; from cold surface to the bath a glass layer, a zone of equiaxial crystals and a zone of columnar crystals are observed. The freeze lining composition only slightly deviates from the bath composition. Furthermore, the authors have observed that the impact of mass transport on the freeze lining growth depends on the morphology of the phase dominating the freeze lining microstructure.

Previous research, however, is only a first step towards understanding freeze lining formation. A full explanation of how the freeze lining forms is not yet given. A next step will be to determine the thermal history of the freeze lining to determine the temperature gradient in the freeze lining and the bath-freeze lining interface temperature during freeze lining formation.

In this article, the freeze lining formation of a synthetic lead slag is studied. Freeze lining microstructures are interpreted using the position and the composition of the phases, equilibration experiments and thermodynamic data to determine the thermal history of the freeze lining.

EXPERIMENTAL

Cooled Probe Technique

The experimental setup is extensively described in previous articles [2, 3, 10]. In the present experiments however an air-cooled probe is used. The experimental procedure is

as follows: 3 kg mixed pure oxide powders are melted in an Al_2O_3 crucible. When the targeted bath temperature (1240°C for the present slag) is reached, a sample of the 'start slag' bath is taken with a cold steel rod and quenched in water. Next, the air-cooled probe with the two fixed thermocouples (at 10 and 20 mm from the probe) is submerged 30 mm into the bath for a fixed time (1, 5, 15, 30, 60 and 120 min) to form a freeze layer. During the experiments the rotational speed of the crucible (28.5 rpm), the air flow rate ($25 \text{ Nm}^3/\text{h}$) and the bath temperature (1240°C) are kept constant. At the end of the experiment, the probe is taken quickly from the slag bath and the freeze layer is quenched in water. Finally an 'end slag' bath sample is taken using the same procedure as for the 'start slag' bath sample.

Equilibration Experiments

The slag bath samples, taken during the probe experiments, are used to perform equilibration experiments. Each sample (0.5 g) is placed in a Pt-crucible held for a fixed time (60 or 120 min) at a constant temperature (700, 800, 900, 1000, 1100 or 1200°C) in air. After the experiment the sample is quenched in water. In these experiments, however, no equilibrium is reached.

Analysis

All samples are analyzed using light optical microscopy (LOM), scanning electron microscopy (SEM) and electron probe micro-analysis (EPMA). For the freeze lining, a sample is taken at the bottom part of the freeze layer. The SEM is used in backscattered electrons (BSE) mode at a 10 kV acceleration voltage. EPMA using wave length-dispersive spectroscopy (WDS) is performed with a reference current of 30 nA in the willemite standard at 20 kV acceleration voltage. As standards, anglesite, willemite, hematite and glaverbel glass are used for Pb, Zn, Fe and Al, Si and Ca respectively.

Thermodynamic Modeling

Thermodynamic calculations are performed with FactSage [1] using the FACT53 and FACToxid thermodynamic databases developed for the Pb- and Zn-containing slag systems [4, 5]. All calculations are performed for a system in equilibrium with air because no reduction agent is present and the slag is continuously in contact with air.

Synthetic Lead Slag

For the experiments, a synthetic lead slag with a composition shown in Table 1 is used. The slag is made by melting pure powders (less than 0.1 wt% impurities). The slag selection is based on its solidification properties predicted with FactSage and not specifically on industrial relevance. A predicted liquidus temperature of 1200°C is selected to combine sufficient kinetics with limited crucible corrosion and PbO fuming. Furthermore, melilite is selected as primary phase because the PbO content in melilite strongly increases with decreasing temperature in this lead slag. Low melting phases such as $\text{Pb}_3\text{Ca}_2\text{Si}_3\text{O}_{11}$ are also wanted to have a temperature indication in the freeze lining. Figure 1 shows the solidification path in air for the selected slag predicted with FactSage. When the slag solidifies, first melilite is predicted to form at 1200°C . At 1160°C spinel

becomes stable and the slag follows the reaction: liquid \rightarrow melilite + spinel. With further cooling $\text{Ca}_3\text{Si}_2\text{O}_7$ forms at 990°C and $\text{PbFe}_{10}\text{O}_{16}$ forms at 980°C following the reactions: liquid \rightarrow melilite + spinel + $\text{Ca}_3\text{Si}_2\text{O}_7$ and liquid \rightarrow melilite + spinel + $\text{Ca}_3\text{Si}_2\text{O}_7$ + $\text{PbFe}_{10}\text{O}_{16}$ respectively. At 930°C the amount of melilite, $\text{Ca}_3\text{Si}_2\text{O}_7$ and $\text{PbFe}_{10}\text{O}_{16}$ decreases when $\text{Pb}_3\text{Ca}_2\text{Si}_3\text{O}_{11}$ and $(\text{Ca,Pb})_2\text{SiO}_4$ get stable following the reaction: liquid + melilite + $\text{Ca}_3\text{Si}_2\text{O}_7$ + $\text{PbFe}_{10}\text{O}_{16}$ \rightarrow spinel + $\text{Pb}_3\text{Ca}_2\text{Si}_3\text{O}_{11}$ + $(\text{Ca,Pb})_2\text{SiO}_4$. Finally all liquid is predicted to solidify at 920°C . Below solidus temperature, around 730°C a following reaction occurs: melilite + $(\text{Ca,Pb})_2\text{SiO}_4 \rightarrow \text{Ca}_3\text{Si}_2\text{O}_7$ + zincite + $\text{Pb}_3\text{Ca}_2\text{Si}_3\text{O}_{11}$.

Table 1: The targeted composition of the synthetic lead slag in weight percent

CaO	SiO ₂	PbO	ZnO	Fe ₂ O ₃
11.7	16.3	50.5	8.3	13.2

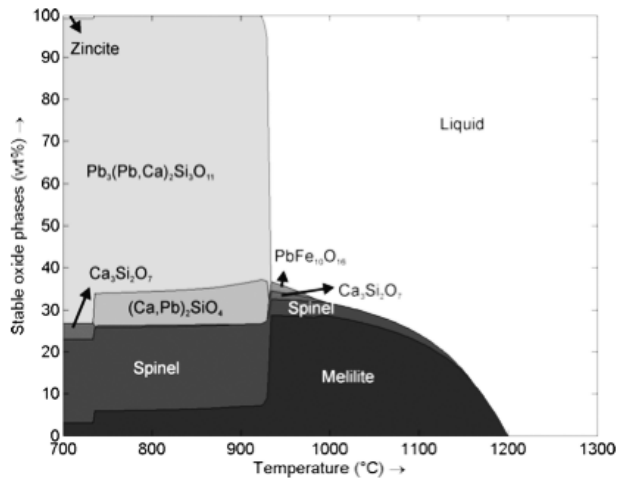


Figure 1: The equilibrium solidification path for the targeted lead slag composition in air predicted with FactSage

RESULTS

Slag Bath Samples

According to analysis of the slag bath sample composition after experiment, only a small contamination of slag (2-4 wt% Al_2O_3) takes place due to dissolution of the crucible. The microstructures of the slag bath samples show that for some experiments melilite and spinel crystals are present in the slag bath. These melilite crystals have a low PbO-concentration.

Thickness Freeze Lining

Figure 2 shows the evolution of the freeze lining thickness in time. The freeze lining grows rapidly, after 5 min the steady state thickness is almost obtained. After 30 min, the changes in freeze lining thickness are limited.

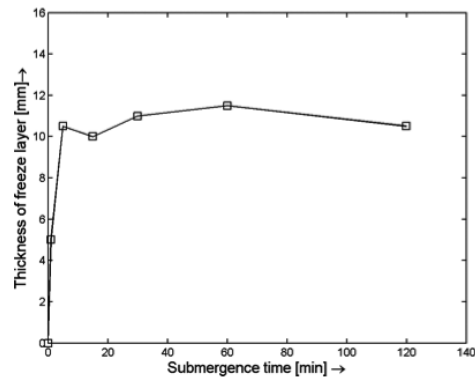


Figure 2: The freeze lining thickness evolution as a function of submergence time

Microstructure Freeze Lining

The microstructure of the freeze lining samples for 1, 15 and 120 min submergence time are shown in Figure 3. After 1 min, four zones can be indicated in the microstructure: a small glass layer at the probe side followed by a zone of a glass layer with crystals, a zone of crystals in liquid phase and at the bath side a layer of remaining slag bath. Melilite is the predominant crystalline phase. Within the melilite crystals, some spinel crystals are entrapped. Between the crystals, glass is observed. This glass was glass or liquid just before quenching of the sample. The reason to distinguish between a zone *with glass with crystals* and a zone *with crystals and liquid* will be explained in the discussion. At longer submergence times, the *crystals with liquid* layer is thicker and after 15 min at the bath side a zone with large interlocked crystals is observed further referred to as sealing crystal layer. Closer to the probe, completely crystallized zone is present between the zone with crystals in glass and the zone with crystals in liquid. Here $Pb_3Ca_2Si_3O_{11}$ and $PbFe$ -silicate crystals are observed between the melilite and spinel crystals. After 120 min only the crystals in the sealing crystals zone are larger when comparing to shorter submergence times.

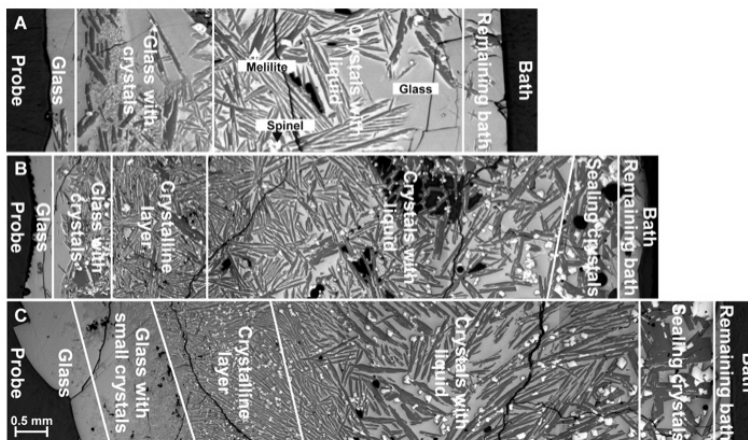


Figure 3: The freeze lining microstructure for A 1 min, B 15 min and C 120 min submergence time

Composition of Glass and Melilite Phases across Freeze Lining

The glass composition strongly changes as a function of distance to the probe as shown in Figure 4a for 120 min submergence time. At the probe side, the glass composition initially equals the bath composition. When small crystals are present (starting at 0.5 mm) the glass composition shows some spread. At 2 mm from the probe the glass composition at once strongly changes: increase in PbO content, decrease in CaO, Fe_2O_3 , ZnO and SiO_2 content. With increasing distance from the probe, the glass composition gradually converges to the bath composition. Between 6 and 10 mm concentration gradients in the glass at the glass-crystal interfaces are observed resulting in a large spread in the glass composition.

The melilite composition also changes systematically with distance to the probe as illustrated in Figure 4b. With increasing distance from the probe, the PbO content decreases while the concentrations of CaO, SiO_2 and ZnO increase. The concentrations of Fe_2O_3 and Al_2O_3 remain approximately constant.

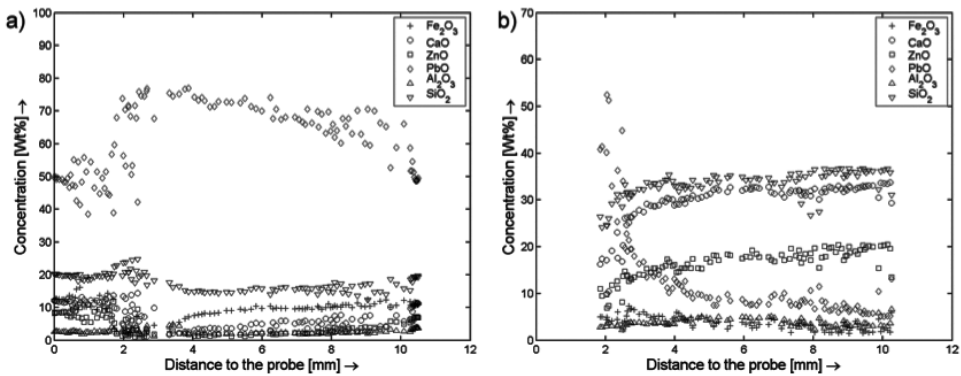


Figure 4: The composition of a) the glass phase and b) the melilite phase as a function of distance to the probe for the 120 min experiment

Equilibration Experiments

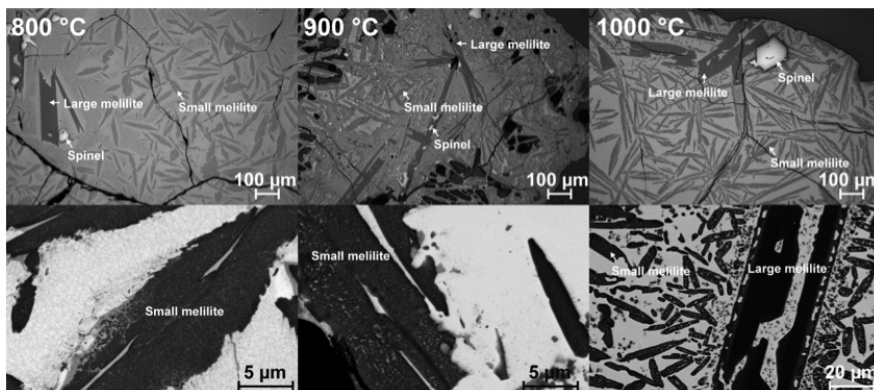


Figure 5: Microstructures of the equilibration experiments of 60 min at 800, 900 and 1000 °C. Above a LOM image is shown and below a SEM image

The equilibration experiments show that below 800 °C the glass crystallizes very slowly.

After 120 min, a limited amount of small crystals formed at 800°C (Figure 5). These crystals are too small to analyze with EPMA, but spinel and melilite crystals could be recognized from the morphology and color. Apart from the small crystals, large melilite crystals with the same composition and morphology as the ones in the slag bath samples are observed. Above 800°C, crystallization happens rather fast. At 900°C, the glass is almost fully crystallized, see Figure 5. Melilite, spinel, $\text{Pb}_3\text{Ca}_2\text{Si}_3\text{O}_{11}$ and PbFe-silicate crystals are observed. Here also large melilite crystals, similar to the ones in the bath samples, are observed, which contained less PbO than the small melilite crystals. Above 900°C, liquid with spinel and small as well as large melilite crystals is observed in the samples. The small melilite crystals contain more PbO than the large one, which are again similar to the ones observed in the bath samples. At 1200°C, only spinel crystals are stable in the liquid. Unfortunately, the small melilite crystals could not be analyzed properly, since liquid and other small crystals are entrapped in the crystals and no homogeneous areas are observed, see Figure 5.

DISCUSSION

Slag

Initially, the slag composition was chosen to have melilite as the primary phase. During the experiments, however, some Al_2O_3 from the crucible is dissolved in the slag bath. As a result spinel is the primary phase and not melilite. This is confirmed with the equilibration experiments. Thermodynamic calculations predict the liquidus temperature of the slag bath to be 1230°C, melilite to be stable below 1160°C and $\text{Pb}_3\text{Ca}_2\text{Si}_3\text{O}_{11}$ to be stable below 860°C.

Freeze Lining Growth

The studied slag easily forms a freeze lining. Already after 5 min the freeze lining thickness is close to its steady state value. Similarly to previous research [2] here zones with different crystal morphology and crystal size are observed in the freeze lining microstructure. After the probe is submerged, first a glass phase layer forms. In this glass layer, some large spinel and large, PbO-poor melilite crystals are entrapped. Because these melilite crystals are similar to those observed in the slag bath samples and because also small, PbO-rich melilite crystals are observed close to the probe, it is concluded that the large crystals were already present in the bath. At the bath side crystals form in the glass layer. If we assume that the freeze lining consists of a solid layer and not of a layer of high viscosity slag, then the growth of these crystals in the liquid determines the further growth of the freeze lining. For the studied slag the growth of the melilite crystals dominates the freeze lining growth, since the melilite phase forms large crystals that do interconnect. Although the spinel phase forms first, its crystals are small, do not interconnect and in the present experimental conditions do not build a layer. When the steady state thickness is reached, the melilite and spinel crystals at the bath side grow large and seal the freeze lining from further interaction with the bath. Between the *glass with crystals and liquid with crystals* layer forms a fully crystalline layer. Here the remaining liquid between the melilite and spinel crystals is consumed to form $\text{Pb}_3\text{Ca}_2\text{Si}_3\text{O}_{11}$ and PbFe-silicate crystals.

Thermal History

Knowing the thermal history of the freeze lining is instrumental in understanding its formation mechanisms. Below, it is estimated using the position of the phases in the freeze lining, the composition of the melilite phase and the composition of the glass phase.

In a first step, the temperature profile established just before quenching the freeze lining is estimated. The equilibration experiments showed that melilite is stable below 1200°C and that $\text{Pb}_3\text{Ca}_2\text{Si}_3\text{O}_{11}$ forms around 900°C. The thermodynamic calculations for the slag bath composition predicted melilite to be stable below 1160°C and $\text{Pb}_3\text{Ca}_2\text{Si}_3\text{O}_{11}$ below 860°C. When assuming the freeze lining composition across the deposit equal to the bath composition, the temperature at the maximum distance to the probe where melilite is present (10.3 mm = r_2) has to be below 1160°C (= T_2) and similarly the temperature has to be below 860-900 °C (= T_1) where $\text{Pb}_3\text{Ca}_2\text{Si}_3\text{O}_{11}$ is present (4 mm = r_1). With this data, the temperature profile is calculated for the freeze lining assuming steady state conditions and a constant value for the heat conductivity coefficient using Equation 1. The assumption that the freeze lining composition equals the bath composition is not valid for the whole freeze lining since at low growth rates of the freeze lining mass transport can result in a mass exchange between bath and freeze lining and thus in a change in freeze lining composition [2]. At a thickness of 4 mm the growth rate of the freeze lining was high (see Figure 2), so here the impact of mass transport was most likely limited. At a thickness of 10.3 mm, the growth rate was slow. However, here the melilite phase was in contact with the bath, so the melilite stability temperature of the bath is taken as an approximation in the present study. The steady state assumption is plausible as during the experiment the temperatures measured at fixed distances to the probe only change slightly after 5 min. For the 120 min experiment, the resulting steady state temperature profile is shown in Figure 6. Furthermore, the equilibration experiments showed that 800°C is the minimum temperature to have intensive crystallization, which is in good agreement with the position of the glass with small crystals-crystalline zone interface. For the 30 and 60 min experiments the steady state profile is similar.

$$T = \frac{T_2 - T_1}{\ln\left(\frac{r_2}{r_1}\right)} \ln\left(\frac{r}{r_1}\right) + T_1 \quad (1)$$

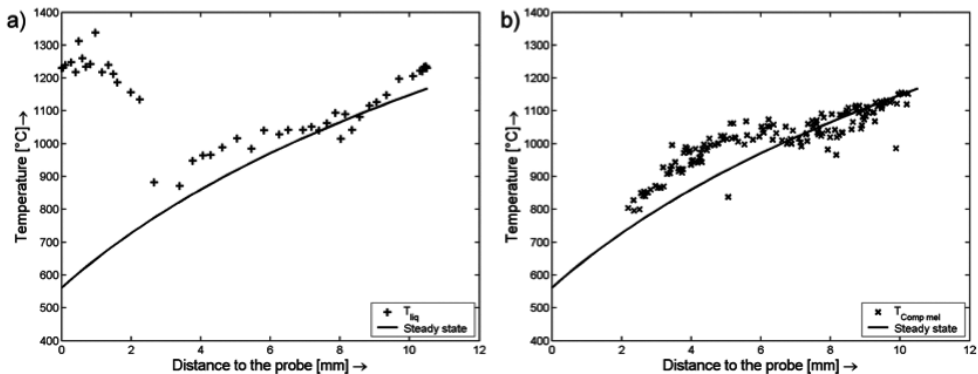


Figure 6: The steady state temperature profile calculated using the position of the phases compared with a) the liquidus temperature profile of the glass phase predicted using FactSage and b) the temperature at which the melilite is stable according to the temperature-melilite composition relation predicted with FactSage using the start bath slag composition as a function of distance to the probe.

An alternative way to estimate the temperature profile just before quenching the freeze lining is by looking at the local liquidus temperature of the glass phase. Because during the experiment, the slag was only cooled down, this liquidus temperature will give a maximum value of the local temperature. Figure 6a shows the resulting liquidus temperature profile predicted with FactSage using the glass compositions shown in Figure 4a. Below 2.5 mm, there is a large difference between predicted glass liquidus temperatures and the steady state temperature profile. Here the local liquidus temperature is close to the bath liquidus temperature. This is the zone where limited crystallization is observed and where the steady state temperature profile gives a temperature below 800°C which is the limit for intensive crystallization. Between 2.5 and 6.5 mm the local liquidus temperature is slightly higher than the steady state temperature profile. Here differences between both profiles might be explained by limited crystallization kinetics because of lower temperatures. Between 6.5 and 9 mm there is a good fit between both profiles. Above 9 mm the local liquidus temperature is again higher than steady state temperature profile. Here the local liquidus temperature gives spinel as primary phase. The freeze lining microstructures, however, show that melilite is already present. Therefore, the temperature has to be below the local liquidus temperature. These results indicate that the estimated steady state temperature profile might be a good estimation of the temperature profile just before quenching the freeze lining.

In a next stage of analysis of results, the freeze lining-bath interface temperature (here further referred to as interface temperature) evolution during the freeze lining formation is estimated. As stated above, the freeze lining growth is determined by the melilite crystal growth for the studied slag. Furthermore the equilibration experiments show that the large melilite crystals observed in the slag bath samples do not change in composition after they formed. Also there is a strong temperature-melilite composition relation. If the assumption that the melilite crystals observed in the sample were formed instantaneously at the freeze lining-bath interface and did not change composition later is correct, then the melilite compositions may be used to estimate the interface temperature as a function of distance to the probe. Because the melilite composition could not be determined properly in the reference experiments, the melilite composition-temperature relation is predicted with FactSage using the start slag bath and therefore, it is assumed that a deviation of the freeze lining composition from the slag bath composition does not result in a change in melilite composition. The resulting estimates of the interface temperature are shown in Figure 6b. The estimated interface temperature does not strongly deviate from the estimated steady state temperature profile. Only at positions below 6 mm, the estimated local temperature is slightly lower than the estimated interface temperature. This indicates that the crystals grow in an undercooled liquid because the steady state temperature profile is almost reached before the melilite crystals form. Note that first a glass layer forms and that a part of the melilite crystals (close to the probe) might be formed in this glass layer and thus not precipitate at the bath-freeze lining interface. Furthermore, note that here we assume the freeze lining to consist of solid material and not of a layer of high viscosity liquid.

Implications for Freeze Lining Application

For freeze lining application, the results indicate that the solidification properties of a slag are important. During freeze lining formation first a glass layer forms. The further growth of the freeze lining is dependent on the growth of the crystalline phases. A crystalline phase that forms an interlocking crystalline framework, which can stabilize the freeze lining, has to be stable between glass transition temperature and liquidus temperature.

For the studied slag, melilite has good freeze lining formation properties since it rapidly forms large crystals that easily interlock forming refractory framework. The spinel phase in this slag seems to have worse freeze lining formation potential since it precipitates in the form of small separate crystals. A proper selection of a slag composition with interlocking crystalline phases is believed to be beneficial to obtain stable freeze lining formation.

Furthermore, the thermal history of the freeze lining indicates that the interface temperature varies between glass formation temperature and liquidus temperature dependent on growth rate of the freeze lining. Initially the freeze lining has a high growth rate as is shown by the thickness evolution in Figure 2 and the interface temperature is close to glass transition temperature (at 2 mm from the probe in Figure 7). With increasing freeze lining thickness, the growth rate decreases and the interface temperature increases. Finally when the steady state thickness is reached, large spinel crystals form at the bath-freeze lining interface. Nevertheless, here also melilite crystals are stable indicating that the interface temperature is still below liquidus temperature.

CONCLUSIONS

The freeze lining formation of a synthetic lead slag has been studied. The results show that the studied slag rapidly forms a freeze lining. For this slag, the growth of the freeze lining is dominated and facilitated by the growth of the interlocking melilite crystals. The spinel phase, although it is the primary phase, forms separated small crystals and is believed to have no stabilization of the freeze lining for the selected slag. Furthermore the thermal history of the freeze linings is studied. The position of the melilite and the $\text{Pb}_3\text{Ca}_2\text{Si}_3\text{O}_{11}$ phase and the local liquidus temperature of the glass phase are used to estimate the steady state temperature profile present just before quenching the freeze linings. The resulting temperature profile gives a bath-freeze lining interface temperature below liquidus temperature. The composition of the melilite phase is used to estimate the bath-freeze lining interface temperature profile. This profile is close to the steady state temperature profile indicating that the heat transfer is much faster than the crystal nucleation and growth and that the crystals form in undercooled liquid.

For freeze lining application the results imply that the solidification properties of the slag are important for fast freeze lining formation. First a glass layer forms on the cooled wall. The further growth of the freeze lining is determined by crystallization. To easily form a freeze lining a phase that forms interconnecting crystals has to be stable above glass transition temperature. Furthermore, the results show that the bath-freeze lining interface temperature varies between glass transition temperature and liquidus temperature during formation of the freeze lining depending on the growth rate of the freeze lining.

REFERENCES

- Bale, C. W., Chartrand, P., Degterov, S. A., Eriksson, G., Hack, K., Ben Mahfoud, R., Melançon, J., Pelton, A. D. & Petersen, S. (2002). *Calphad*, Vol. 26 (2), pp. 189-228. www.factsage.com. [1]
- Campforts, M., Verscheure, K., Boydens, E., Van Rompaey, T., Blanpain, B. & Wollants, P. (2007). *Metall. Trans. B*, Vol. 38B(6), pp. 841-51. [2]
- Campforts, M., Verscheure, K., Boydens, E., Van Rompaey, T., Blanpain, B. & Wollants, P. (2008). *Metall. Trans. B*, Vol. 39B(3), first online. [3]

- Decterov, S., Jung, I. H., Jak, E., Hayes, P. & Pelton, A. D.** (2004). Proc. VII Int. Conf. on Molten Slags, Fluxes and Salts, Cape Town, South Africa, SAIMM, Johannesburg, South Africa, pp. 839-50. [4]
- Jak, E., Decterov, S., Zhao, B., Pelton, A. D. & Hayes P. C.** (2000). Metall. Trans. B, Vol. 31B, pp. 621-30. [5]
- Pistorius, P. C.** (2004). Proc. VII Int. Conf. on Molten Slags, Fluxes and Salts, Cape Town, South Africa, SAIMM, Johannesburg, South Africa, pp. 237-42. [6]
- Pistorius, P. C.** (2003). J. S. Inst. Min. Metall., Vol. 103 (8), pp. 509-14. [7]
- Solheim, A. & Støen, L. I. R.** (1997). Light Metals 1997, Orlando, FL, TMS, Warrendale, PA, pp. 325-32. [8]
- Thonstad, J. & Rolseth, S.** (1983). Light Metals 1983, New York, NY, TMS-AIME, Warrendale, PA, pp. 415-23 [9]
- Verscheure, K., Campforts, M., Verhaeghe, F., Boydens, E., Van Camp, M., Blanpain, B. & Wollants, P.** (2006). Metall. Trans. B, Vol. 37B(6), pp. 929-40 [10]
- Zietsman, J. H. & Pistorius, P. C.** (2006). Minerals Engineering, Vol. 19, pp. 262-79 [11]

